Geologia Croatica
Journal of the Croatian Geological Survey and the Croatian Geological Society
2018 | 71/1 | 19–28 | 8 Figs. | 3 Tabs. | www.geologia-croatica.hr

A mineralogical and petrographic study of evaporites from the Mali Kukor, Vranjkovići, and Slane Stine deposits (Upper Permian, Dalmatia, Croatia)

Željko Dedić*, Nikolina Ilijanić and Slobodan Miko

Croatian Geological Survey, Sachsova 2, P.O. Box 268, HR-10000 Zagreb, Croatia
(*corresponding author: zdedic@hgi-cgs.hr)

doi: 10.4154/gc.2018.02

Article history:
Manuscript received August 09, 2017
Revised manuscript accepted December 20, 2017
Available online February 28, 2018

Abstract

The evaporite deposits examined in this study are located in the central part of middle Dalmatia, Croatia. In this region, Upper Permian evaporite sediments were deposited under favourable conditions onto the Variscan basement around the northern margins of Gondwana. These sediments can be subdivided into three members, a lower evaporite unit (an anhydrite member), a middle evaporite unit (a gypsum member), and an upper unit (a clastic member), and are mainly comprised of secondary gypsum that formed via the hydration of precursor anhydrite rocks. The middle evaporite unit comprises beds of gypsum as well as early diagenetic dolomites that contain gypsum sequences, extending up to 60 m maximum thickness, and overlying clastic sequences that themselves are up to 20 m thick. These Upper Permian evaporite sediments contain horizontal, irregular, gypsum lithofacies that exhibit pronounced enterolithic and boudinage structures. The characteristics of these sediments are indicative of deposition in supratidal and sabkha settings (i.e., early diagenetic dolomites and evaporites) within a shallow epicontinental marine environment with highly varied coastlines, bays, and lagoons. The secondary gypsum seen within this Upper Permian middle evaporite unit displays alabastrine and porphyroblastic secondary textures and includes corroded anhydrite relics; associated minerals include muscovite, chlorite, potassium (K)-feldspar, quartz, and amphibole. The Upper Permian evaporite sediments discussed in this study are composed of irregular, locally brecciated secondary gypsum that probably formed as a result of multiple synsedimentary collapse of pre-existing soluble minerals and/or synsedimentary and post-sedimentary tectonics.

Keywords: Upper Permian, Evaporite sediments, Gypsum, Anhydrite, Dalmatia

1. INTRODUCTION

Gypsum is by far the most abundant secondary mineral in sedimentary settings, sometimes forming the calcium sulfate mineral anhydrite in arid and hot supratidal environments (sabkhas) in the presence of concentrated brines, but rarely at the surface (KINSMAN, 1966; BUTLER, 1969; SHEARMAN, 1985; STROHMENGER et al., 2008; ZAKI et al., 2011; ABRANTES et al., 2016).

Gypsum is readily prone to dehydration, producing water and anhydrite, when heated to a temperature that is high enough as a function of the salinity of coexisting fluids (HARDIE, 1967; AZIMI et al., 2011; MA et al., 2015). Thus, the most common process that causes the dehydration of gypsum, and thus the formation of anhydrite, is burial to depths below the reaction isotherm, in settings where fluids can still escape the system. If anhydrite is uplifted back above the reaction isotherm, it can return to gypsum, provided sufficient water is available. Ancient evaporites are economically important sources of salts (e.g., gypsum) and metals (e.g., Cu, Zn, and Au), as well as being key indicators for the existence of structural oil and gas traps (WARREN, 2006).

Upper Permian evaporite deposits occur in the Dinarides in central Dalmatia (TIŠLJAR, 1992) and can be observed at a number of sites. Three known sites in this region that contain evaporite deposits were formerly active quarries for the extraction of gypsum and are thus the focus of this study: the Mali Kukor quarry in Kosovo polje, Vranjkovići quarry near Vrlika, and the Slane Stine quarry near Sinj. The aim of this study is to highlight the depositional environments and phases of diagenetic evolution that led to the formation of these Upper Permian evaporites based on the results of petrographic and sedimentological investigations of beds within the sequences at these sites.

The Upper Permian evaporites and adjacent sediments known from middle Dalmatia have been the subject of extensive geological investigations in the past (TIŠLJAR, 1992, ŠUŠNJARA et al., 1992, GABRIĆ et al., 2002). Previous studies have addressed the age of these sequences, their superposition and tectonic relationships with surrounding rocks, their mineralogy, petrology, and chemical composition, and have determined the conditions and environments of their deposition.

The most comprehensive resource available regarding the geology of this area is the basic geological maps of the Republic of Croatia at a 1:100,000 scale, specifically the Knin, Drniš, and Sinj sheets (GRIMANI et al., 1962–1966; PAPEŠ et al., 1962–1966; GRIMANI et al., 1975; IVANOVIĆ et al., 1977; IVANOVIĆ et al., 1978; RAIĆ et al., 1984). These deposits have also been extensively studied in order to calculate the extent of gypsum reserves as a mineral commodity; this research has generated detailed site data based on exploration drilling and core analyses (LUKŠIĆ et al., 2005).

The Upper Permian evaporites and adjacent sediments known from middle Dalmatia were deposited above a Variscan basement in hypersaline marine and/or marine-marginal deposi-

tional settings around the margins of northern Gondwana (TIŠLJAR, 1992). The upper part of the Middle Permian as well as the Upper Permian in this region is characterized by the formation of carbonates, notably dolostones and some sabkha evaporites (VLAHOVIĆ et al., 2005). Evaporitic rocks within deposits at the Kosovo polje were previously studied by KULUŠIĆ & BOROJEVIĆ ŠOŠTARIĆ (2014) and considered to be part of the Dinaric evaporite mélange.

The aim of this study is to highlight the origins of Upper Permian evaporite depositional environments and to discuss their diagenetic evolution based on petrographic and sedimentological investigations of carbonates and evaporites at a series of study sites.

2. GEOLOGICAL SETTING

The study area and deposits discussed in this paper are located in middle Dalmatia, Croatia (Fig. 1), within the central part of the outer Dinarides. The Dinarides generally encompass a stratigraphic range between the Middle Permian (or even the Upper Carboniferous) and the Eocene (TIŠLJAR et al., 1992; VELIĆ et al., 2002a; VLAHOVIĆ et al., 2005).

It is thought that deposits ranging from the top of the Lower Jurassic (Toarcian) to the top of the Cretaceous can be attributed to the Adriatic Carbonate Platform (AdCP), one of the largest Mesozoic structures of this type within the peri-Mediterranean region (DERCOURT et al., 1993, 2000; VLAHOVIĆ et al., 2005).

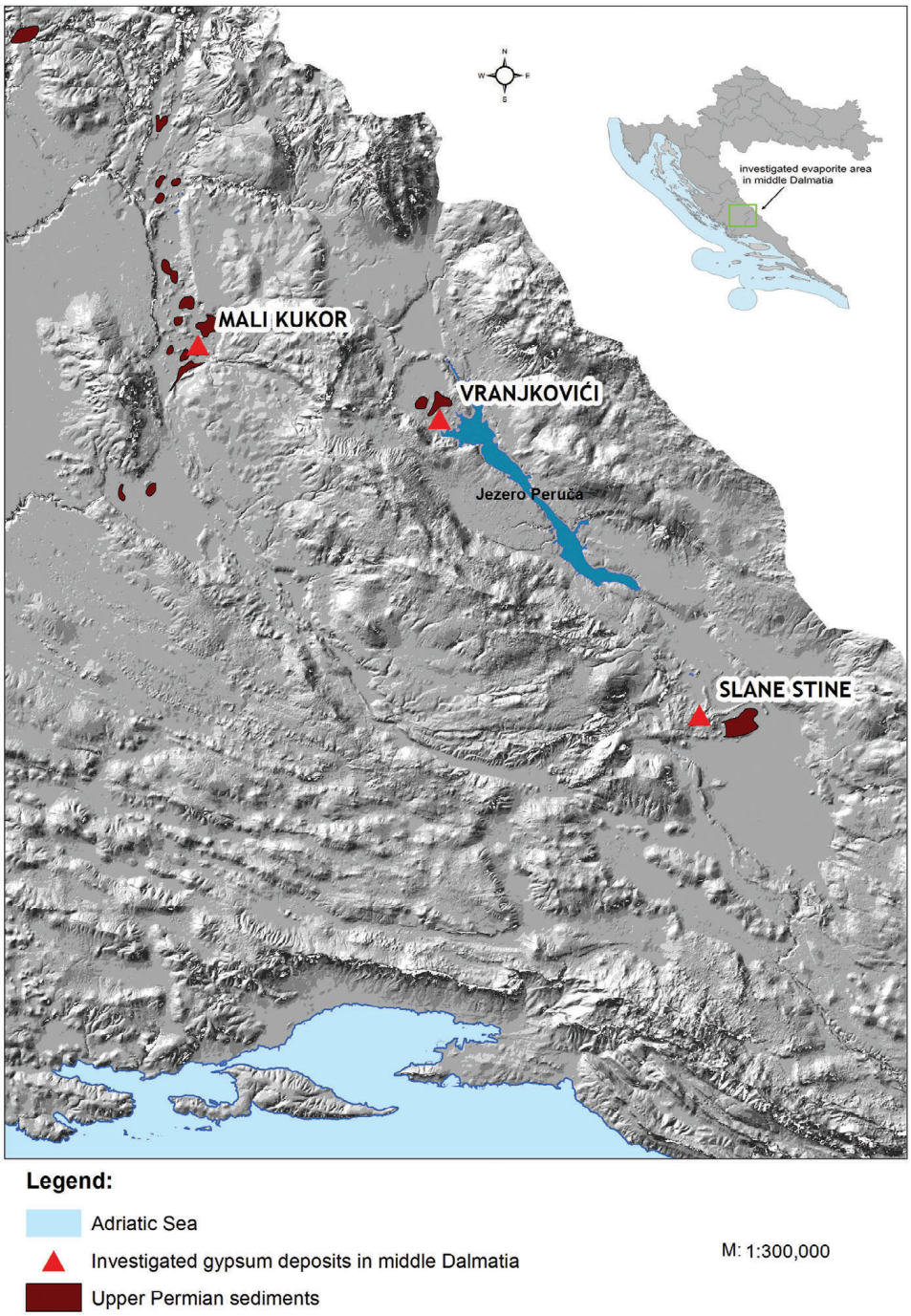

Figure 1. Map to show the locations of the study sites in middle Dalmatia, Croatia. The reference source for Upper Permian sediments used in this paper is the 1:300.000 Geological Map of the Republic of Croatia (CGS, 2009).

The basement of the AdCP can be subdivided into several major sequences, the oldest of which encompass Upper Carboniferous to Middle Permian rocks and comprise part of the Variscan basement. Siliciclastic deposition prevailed during the Carboniferous period followed by mixed clastic-carbonate deposits in the Lower Permian and a transition within the Lower/Middle Permian into continental clastic deposition.

Similarly, the Middle Permian to Middle Triassic sequence in this region is characterized by carbonate and mixed siliciclastic-carbonate deposits that formed an epeiric platform at this time along the northern margin of Gondwana, while the upper part of the Middle Permian and Upper Permian is characterized by carbonates and sabkha evaporites (VLAHOVIĆ et al., 2005).

Ancient epeiric evaporitic platforms (SHAW, 1964; IRWIN, 1965; WETZEL et al., 2013; ORTI et al., 2017) are huge areas of restricted stagnant circulation on the continental margins of seaways where extensive evaporite beds periodically accumulated (WARREN, 2006).

The Upper Permian sequences of middle Dalmatia comprise three main facies types, carbonates (mainly limestones), evaporites (gypsum and anhydrite), and early diagenetic dolomites and clastics including siltstones, sandstones, and rare conglomerates. Exceptional facies types in this region include porous carbonate cavity breccias, so-called "rauchwackes" (ŠUŠNJARA et al., 1992; TIŠLJAR, 1992).

3. METHODS

A series of detailed field investigations of Upper Permian evaporite units were carried out at the Mali Kukor, Vranjkovići, and Slane Stine sites (Fig. 1). A total of 45 representative samples were selected from processed profiles and subjected to further laboratory analysis; thin sections for mineralogical-petrographic analysis were prepared from all samples, and 24 bulk evaporite samples were selected for X-ray diffraction (XRD) analysis.

Preparation of evaporite thin sections required the use of a special method. Samples were first crushed and hand ground with a pestle and mortar before a few grams of each were sieved through a 125 mesh section. Cutting, polishing, and thinning were then carried out using Norland Optical Adhesive 61, glue that hardens under ultraviolet light. All of the thin sections were then examined using a polarizing microscope.

Bulk sample mineral compositions were determined using a PANalytical X'Pert Powder X-ray diffractometer equipped with Ni-filter Cu Kα radiation, a vertical goniometer with θ/θ geometry, and a PIXcel detector. Scans were performed at 45 kV and 40 mA using both a ¼ divergence slit and anti-scatter slits and with a step size of 0.002° 2θ every four seconds across a range between 4° 2θ and 66° 2θ. Individual minerals were identified on the basis of their reflections following the method outlined by MOORE & REYNOLDS (1997); semi-quantitative mineral analysis was performed using the software RockJock (EBERL, 2003), and the weight percent (wt %) of minerals in each sample was calculated using integrated X-ray intensities.

4. RESULTS AND DISCUSSION

4.1. The lithofacies at Mali Kukor, Vranjkovići, and Slane Stine

Detailed field observations enabled the identification of three distinct lithofacies within the quarries, evaporites, carbonates and clastics i.e., siltstones, sandstones and carbonate cavity breccias.

The dominant lithofacies in the Slane Stine quarry comprise anhydrite in the lower part of the profile with clasts that range in size between 1 – 5 cm diameter. This basal sequence is around 25 m thick and occurs beneath an alternating sequence of anhydrite, dolomite, and massive gypsum that marks the middle of the plateau. This overall sequence is then capped by an approximately 15 m thick tectonic zone that comprises green and reddish clastic sediments. The lithofacies within the Slane Stine quarry also includes fragments of carbonate rocks (dolomites) within evaporative (gypsum) sediments that are characterized by enterolithic folding (Fig. 2).

The lithofacies in the Vranjkovići quarry include poorly developed horizontal laminations of secondary gypsum with dolomite intercalations that contain organic matter in their lower portions. These can be up to 15 m thick and underlie an alternating sequence of massive gypsum units including thinly bedded early diagenetic dolomite (ca. 5 m thick) below palaeokarst forms (Fig. 3).

The lithofacies in the Mali Kukor quarry comprise dolomites and alternating thinly bedded white and gray gypsum units that contain portions of dolomitic breccia in their lower parts. These units are up to 20 m thick, occurring below a zone of alternating

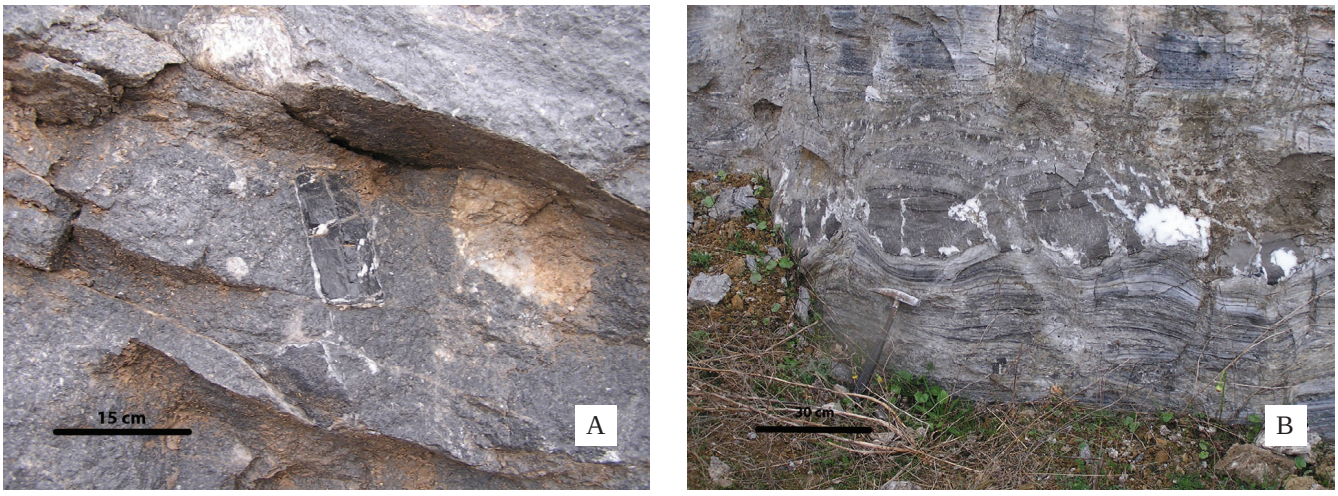

Figure 2. (A) Fragments of carbonate rocks (dolomites) within evaporitic (gypsum) sediments in the Slane Stine near Sinj. (B) An example of enterolithic folding within the Slane Stine deposit.

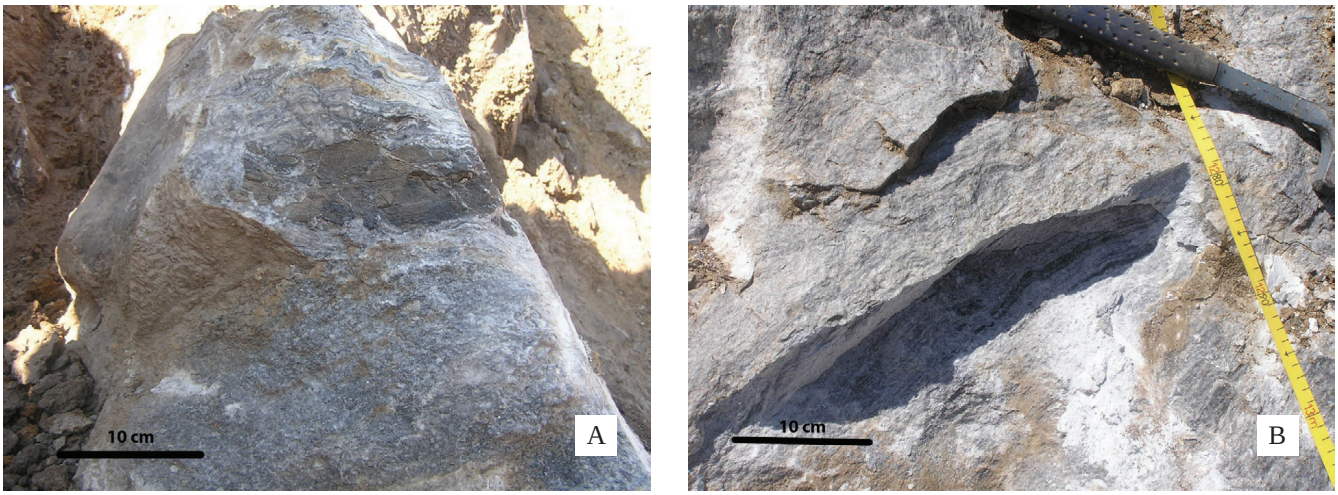

Figure 3. (A) Images from the top of the geological profile at Vranjkovići showing the alternation between massive gypsum and thinly bedded early diagenetic dolomite that terminates in palaeokarst structures. (B) The lower part of the geological profile at Vranjkovići showing poorly developed horizontal laminations of secondary gypsum and dolomite intercalations.

secondary gypsum and anhydrite, which terminates in green and reddish clastic deposits (Fig. 4).

In summary, the following basic lithofacies are seen at all three sites:

- A laminated evaporite-carbonate facies composed of millimetre-centimetre-sized gypsum and anhydrite laminae intercalated with dolomite and dolomicrite and organic matter patches. This facies type is also characterized by horizontal, wavy, and irregular laminations as well as enterolithic, massive, and boudinage-style lithologies;
- An evaporite-carbonate breccia facies that is composed of millimet-metre-sized fragments of dolomite and anhydrite relics.

The laminated evaporite-carbonate facies also presents a series of very thin evaporite beds and laminae interbedded, or interlaminated, with thinner, dark, lime, muddy structures that contain organic material (possibly algal mats) and thinly bedded dolomites. These evaporite laminae range in thickness from 0.1 mm upwards and often disintegrate into fine-grained dolomicrite and dolomite, organic matter, or anhydrite. Evaporite laminae within the sections studied in this paper also display enterolithic and boudinage features forms of dolomite or organic matter patches intercalated with evaporite laminae.

Evaporite-carbonate breccia facies containing fragments of dolomite or anhydrite relics are seen at all three sites; this lithofacies type consists of angular or irregular fragments of various sizes set within a sulfate groundmass.

4.2. A mineralogical and petrographic evaluation of the evaporites

A microscopic mineralogical-petrographic study was carried out on the laminated evaporite-carbonate facies described above that comprises millimetre-to-centimetre scale gypsum and anhydrite laminae intercalated with dolomites, dolomicrites, and organic matter. The results of this investigation show that the Upper Permian evaporite units from all three sites discussed in this paper are primarily composed of microcrystalline secondary gypsum. Samples from all three deposits nevertheless display a variety of textures ranging from xenotopic to idiotopic and encompass four types of secondary gypsum:

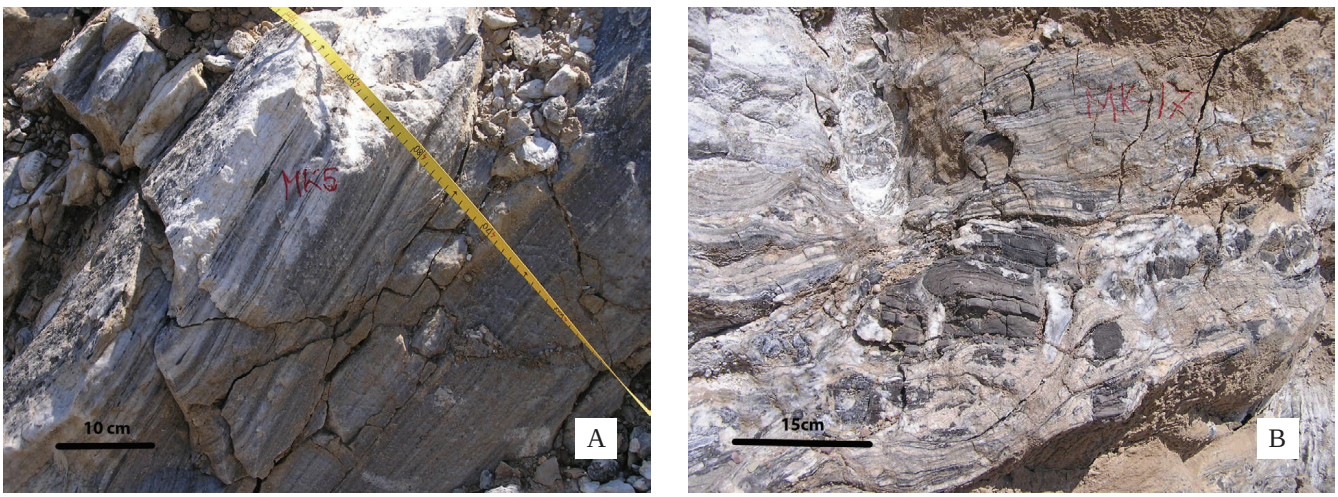

Figure 4. The lower zone of the geological profile at Mali Kukor showing alternating thinly bedded white and gray gypsum and organic patches that possibly represent algal mats (A). The upper zone of the geological profile at Mali Kukor showing organic patches and anhydrite embedded within a gypsum mass (B).

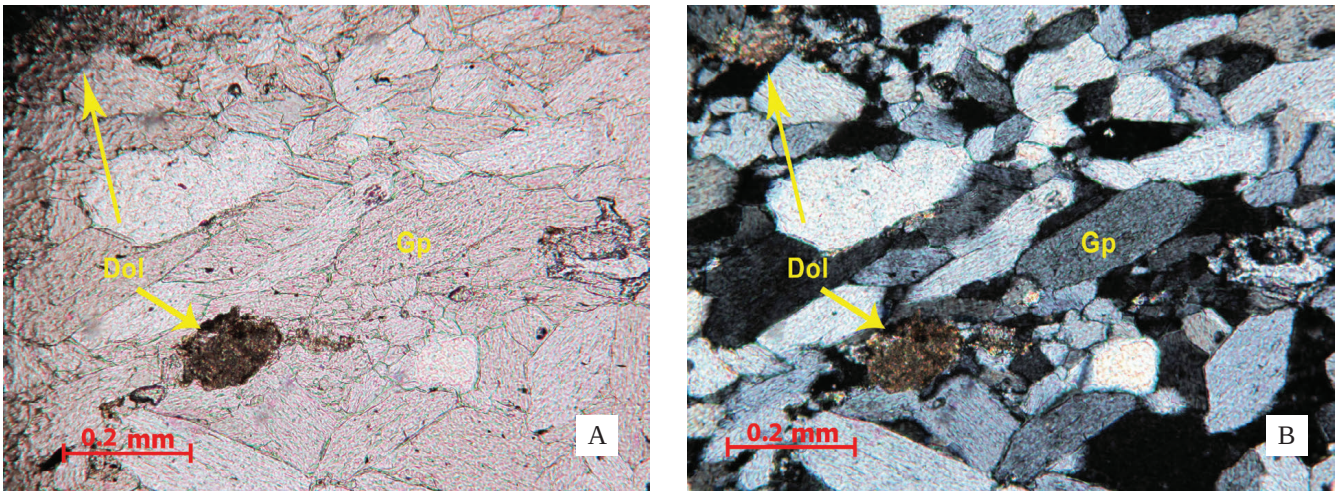

Figure 5. Thin-section images of sample Mk-12, an alabastrine secondary gypsum that contains euhedral-to-subeuhedral features around 200 μm in size. Most of the oriented crystals within this sample are relics of fine-grained crystallized secondary dolomite (Dol) as well as coarse-grained crystallized secondary dolomite (Dol). The image on the left (A) is under plane-polarized light while the one on the right (B) is under cross-polarized light).

(1) Alabastrine;
(2) Porphyroblastic;
(3) Fibrous satin spar, and
(4) Granoblastic.

Within these varieties, fibrous satin spar gypsum is the only type formed from sulfate-rich solutions that develop due to anhydrite hydration; all the other varieties form via the rehydration of an anhydrite precursor. The mineral abbreviations used in the subsequent text and figures are as outlined by KRETZ (1983).

Observations show that secondary gypsum is the most widespread form seen in Upper Permian evaporite units at the three sites. This kind of gypsum can be classified into several forms which can be loosely grouped into three stages that comprise a continuous recrystallization sequence. Thus, in stage 1, alabastrine secondary gypsum directly forms from anhydrite, contains abundant corroded inclusions, and comprises a mosaic of complex, interlocking anhedral grains that about one another to such an extent that their grain boundaries are almost impossible to trace. Viewed under crossed poplars, each grain appears fibrous and ill-defined and exhibits an irregular undulating extinction. The bulk of this type of gypsum appears to have been formed at, or very near, the surface as it develops via the weathering of anhydrite outcrops.

When no anhydrite relics are present in stage 1 gypsum, recrystallization is initiated to form stage 2 or stage 3 granoblastic gypsum. This form is not seen adjacent to anhydrite as it does not form from this starting point.

Stage 2 gypsum comprises small, usually anhedral, grains that are characterized by non-undulatory extinction, sometimes with curved re-entrant boundaries. The grain size of this form is usually uniform, with diameters around 50 μm, and the presence of larger subhedral and euhedral crystals are indicative of further recrystallization to stage 3. Thus, stage 3 gypsum, which develops from either stage 2 forms or directly from stage 1, is composed of subhedral or euhedral grains about 100 μm in diameter. It is noteworthy that the grain size of this form can be variable, reaching up to 0.5 mm in diameter; many larger grains can be blasts that contain no anhydrite relics, and have well-developed crystal faces and textures that formed subsequent to the finer gypsum matrix (HOLLIDAY, 1970).

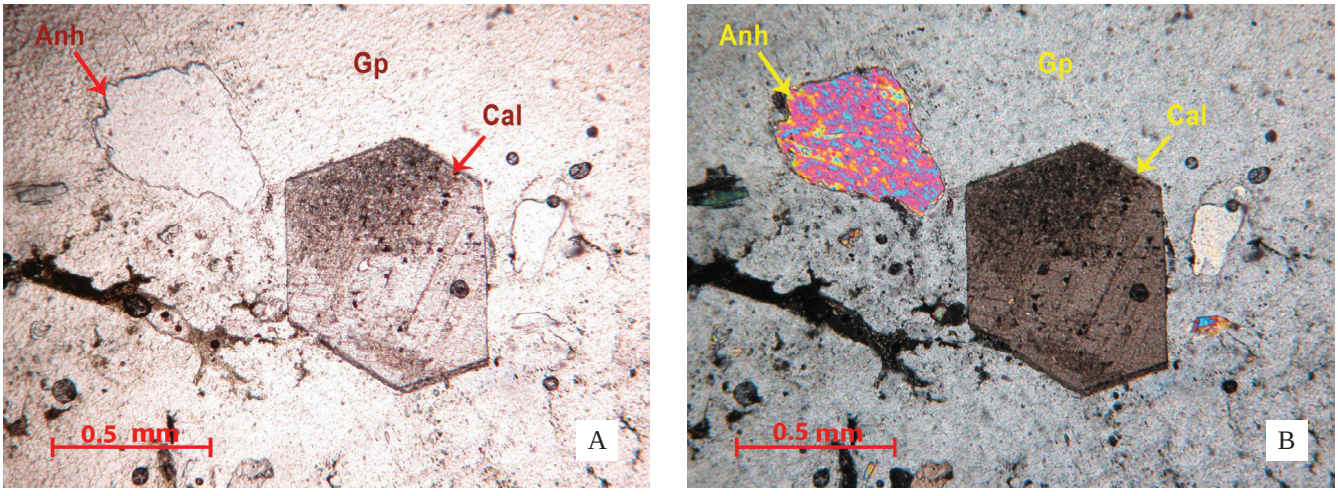

Figure 6. Thin-section images of sample Mk-16, a porphyroblastic secondary gypsum that contains inclusions of carbonates, dolomites, and calcite (Cal), as well as corroded anhydrite relics (Anh). The image on the left (A) is under plane-polarized light while the one on the right (B) is under cross-polarized light.

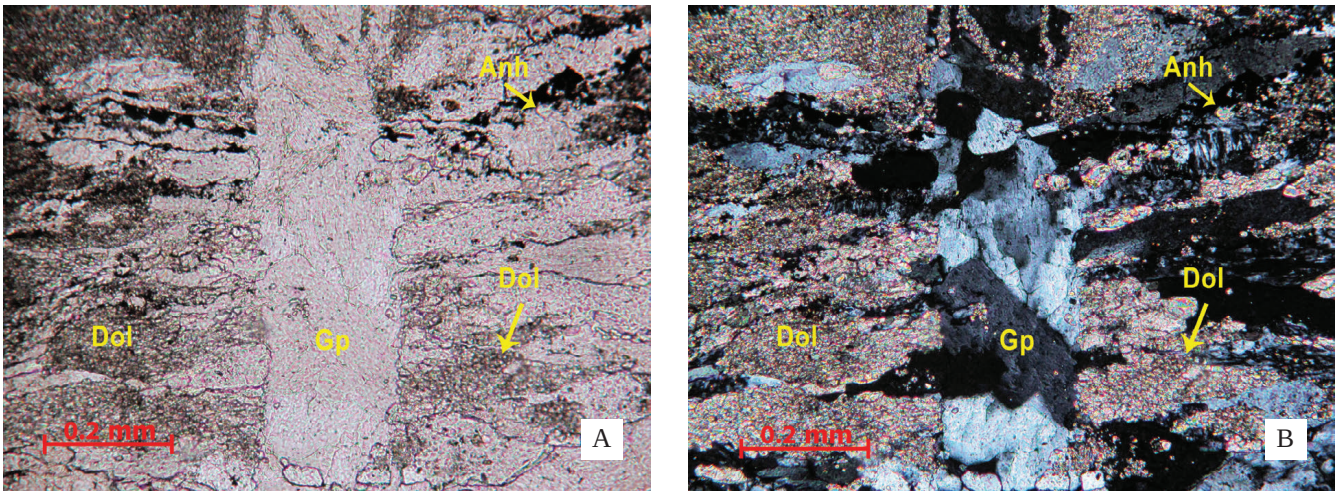

Figure 7. Thin-section images of sample Mk-5c, gypsum veins within a dolomite intraclast (Dol) and a mineral assemblage from the evaporite facies. These images show an anhydrite (Anh) relic floating within subhedral crystals of gypsum (Gp). The image on the left (A) is under plane-polarized light while the one on the right (B) is under cross-polarized light.

Microscopic thin sections reveal that the textures of alabastrine gypsum can exhibit erratic and migrating extinction shadows when samples are rotated under cross-polarized light (Fig. 5). Examples of this gypsum with euhedral-to-subeuhedral features comprises the most frequent crystal orientations within the samples examined in this study alongside relics of fine-grained crystallized secondary dolomite (Fig. 5). Indeed, as these secondary gypsum crystals were most probably formed from anhydrite they can vary from place to place. In early work, OGNIBEN (1957) discussed super-individual examples of alabastrine secondary gypsum that comprise sub-crystals with shadowy grain boundaries as well as the extinction polarization of aggregates of microcrystalline gypsum less than 70 μm in diameter. The crystal size of samples from the Mali Kukor site (sample Mk-12) is around 200 μm, and alabastrine gypsum can include a wide range of related textures which all form a natural grouping, in contrast to the porphyroblastic variety. The crystals of alabastrine gypsum are therefore commonly circular, irregular, or form elongated patches adjacent to, or within, the porphyroblastic form. The boundaries between the finer-grained alabastrine form and its coarser counterpart also tend to exhibit gradational interpenetrating contacts indicative of the replacement of larger gypsum crystals by smaller ones. This process of degradation has been described in Miocene evaporites from the Red Sea (AREF, 2003), from Messinian evaporites in Italy (TESTA & LUGLI, 2000), and in pedogenic gypsum crusts (WATSON, 1988; AREF, 2003).

In contrast, porphyroblastic gypsum tends to forms both large and small crystals that have generally interlocking margins. In some examples the individual crystals are clearly defined, while in other cases samples can be very coarsely crystalline (Fig. 6). Porphyroblastic gypsum therefore comprises large, anhedral porphyroblasts up to 1 cm in length that tend to occur as single crystals, although aggregates can also be locally abundant. This form also contains numerous inclusions of corroded anhydrite relics or other associated minerals, and porphyroblasts are surrounded by later alabastrine secondary gypsum, often the stage 3 granoblastic form. Other associated minerals can include anhydrite, dolomite, muscovite, chlorite, amphibole, potassium (K)-feldspar, apatite, rutile, and quartz, while pyrite and organic material are also common in some samples. Hydration veins are also common features of these secondary lithofacies and are often filled with satin spar gypsum (Fig. 7). Observations show that gypsum porphyroblasts do not form to any great extent in present-day anhydrite settings where the alabastrine type is dominant, indicating that these structures are components of an earlier phase of gypsification. This conclusion is corroborated by the fact that similar porphyroblasts have been recorded as comprising the earlier form of secondary gypsum in many areas (FORBES, 1958; HAM, 1962; WEST, 1964). This kind of gypsum is composed of large euhedral-to-subhedral crystals that exhibit sharp extinction and occur as individual elements or in groups of two or three crystals. HOLLIDAY (1970) and TAJ (2012) noted that the origin of porphyroblastic gypsum via anhydrite rehydration was evidenced by corroded anhydrite relics in samples from the three sites they investigated (Fig. 6).

The fibrous (satin spar) gypsum variety is the only type that forms from sulfate-rich solutions, developed due to the rehydration of anhydrite; all other known types of secondary gypsum form via the rehydration of precursor anhydrite (MAKLOUF et al., 2006). The formation of satin spar gypsum is therefore thought to be the result of the increase in volume that characterizes the transformation of anhydrite to gypsum (SHEARMAN et al., 1972; YEŞİLOVA & HELVACI, 2013). Thus, prismatic anhydrite laths are often observed as pseudomorphs within host sediment; for example, fibrous (satin spar) gypsum occurs as veins interbedded within evaporites and within the carbonates of the Abu Ruweis Formation (MAKLOUF et al., 2006). Similarly, veins from sample Mk-5c (Fig. 7) are composed of elongate crystals arranged perpendicular to walls; in this case, veins of fibrous (satin spar) gypsum are interbedded within a dolomite intraclast and comprise an evaporite facies mineral assemblage in thin section. Fibrous (satin spar) gypsum is composed of crystals greater than 200 μm in length, while relic anhydrite components greater than 10 μm in size also float within subhedral gypsum crystals that can also sometimes be arranged randomly. It is therefore thought that such randomly oriented crystal veins were originally formed from anhydrite at depth and at high temperatures and pressures, before subsequently being rehydrated to gypsum. A number of previous authors have considered satin spar gypsum to therefore be a by-product of anhydrite rehydration (SHEARMAN et al., 1972; TESTA & LUGLI, 2000).

Granoblastic gypsum has a limited distribution within the Upper Permian evaporite units discussed in this study, recorded in only the Mali Kukor and Vranjkovići deposits. This form ex-

Table 1. Bulk semi-quantitative mineralogy of evaporite samples from the Slane Stine site.

Sample	Gypsum	Anhydrite	Dolomite	Muscovite	Chlorite	Amphibole	K-feldspar	Apatite	Rutile	Quartz
SS-2	83	7	1	8	–			1		–
SS-3A	86	4	2	8	–	–	–	–	–	–
SS-6A	76	5	3	12	3	–	–	–	1	–
SS-12A	63	–	3	14	7	1	9	–		3
SS-PIR	30	–	60	7	–	3	–	–	–	–

Table 2. Bulk semi-quantitative mineralogy of evaporite samples from the Mali Kukor site.

Sample	Gypsum	Calcite	Dolomite	Amphibole	Quartz	Muscovite	Celestine	Apatite	Anhydrite
MK-3	15	83	–	–	1	–	–	1	–
MK-5B	97	–	–	2	–	–	–	1	–
MK-8	80	12	–	2	3	–	3	–	–
MK-12	97	–	–	2	1	–	–	–	–
MK-14	88	5	–	2	1	4	–	–	–
MK-16	88	–	3	2	–	7	–	–	–
MK-ANH	67	–	–	2	–	–	–	–	31

hibits well-defined euhedral-to-subhedral crystals that have sharp and homogenous extinction patterns. Such crystals are almost equigranular in size, range between 10 μm and 50 μm, interlock with one another, and form mosaic textures. These granular crystals also exhibit dominantly euhedral faces toward porphyroblastic gypsum, indicative of a replacement origin, and this secondary type is also characterized by the absence of anhydrite relics. It is therefore thought that granoblastic gypsum represents an advanced stage of anhydrite rehydration (WEST, 1964, 1965; HOLLIDAY, 1970; WARREN, 1999, MAKLOUF & EL-HADDAD, 2006, TAJ, 2012).

On the basis of the petrographic descriptions presented in this study, it is clear that the Upper Permian gypsum evaporites from selected sites across middle Dalmatia are mainly composed of secondary gypsum that most probably originated from either the hydration (by groundwater) of and/or the surface weathering of precursor anhydrite rocks. It is noteworthy in this context that the term "secondary gypsum" was first used by MURRAY (1964) and then later by HOLLIDAY (1970) and SHEARMAN (1972) to refer to gypsum that formed via hydration of anhydrite.

4.3. The bulk mineralogy of evaporite samples

The results of bulk XRD analysis of 24 samples (Tabs. 1–3) shows that the dominant mineral components are gypsum, dolomite, and anhydrite, while calcite, chlorite, K-feldspar, muscovite, quartz, amphibole, and apatite also occur in smaller proportions. Celestine and rutile were detected in just one sample from the Mali Kukor site (sample MK-8).

Mineral compositions at the Slane Stine site are dominated by gypsum, anhydrite, and muscovite, with the exception of samples SS-12A and SS-PIR which do not contain anhydrite (Tab. 1). Dolomite is also present in most cases in minor concentrations, but is the dominant phase (alongside gypsum) in sample SS-PIR, while apatite, rutile, and quartz also occur in minor amounts.

Gypsum is the dominant mineral phase in all samples from the Mali Kukor site (Tab. 2; Fig. 8), while anhydrite was seen in just one sample (MK-ANH) from this site, and calcite is present in samples MK-3, MK-8, and MK-14. Mineral phases that appear in minor concentrations in the samples from this site include amphibole, quartz, and muscovite (in samples MK-14 and MK-16), while dolomite is only seen in sample MK-16, celestine is only observed in sample MK-8, and hydroxylapatite is only seen in samples MK-3 and MK-5B.

All the samples from the Vranjkovići site contain both gypsum and dolomite as their main mineral phases (Tab. 3), while minor amounts of amphibole are also present in nearly all samples (with the exception of VR-6), alongside muscovite in samples VR-11, VR-12, VR-13, and VR-14, K-feldspar in samples VR-5-2, VR-11, VR-12, VR-13, and VR-14, apatite in samples VR-5-1 and VR-5B, and anhydrite in sample VR-11.

The microscopic and XRD investigations of Upper Permian evaporite samples discussed here reveal the presence of carbonates

Table 3. Bulk semi-quantitative mineralogy of evaporite samples from the Vranjkovići site.

Sample	Gypsum	Dolomite	Amphibole	Apatite	K-feldspar	Muscovite	Anhydrite
VR-5-1	87	11	1	1	–	–	–
VR-5-2	68	25	1	–	6	–	–
VR-5B	79	19	1	1	–	–	–
VR-6	97	3	–	–	–	–	–
VR-6B	97	1	2	–	–	–	–
VR-9A	99	–	1	–	–	–	–
VR-11	90	–	1	–	3	5	1
VR-12	79	6	1	–	7	7	–
VR-13	69	22	2	–	4	3	–
VR-14	66	23	2	–	4	5	–
VR-15	94	4	2	–	–	–	–
VR-18	50	50	–	–	–	–	-

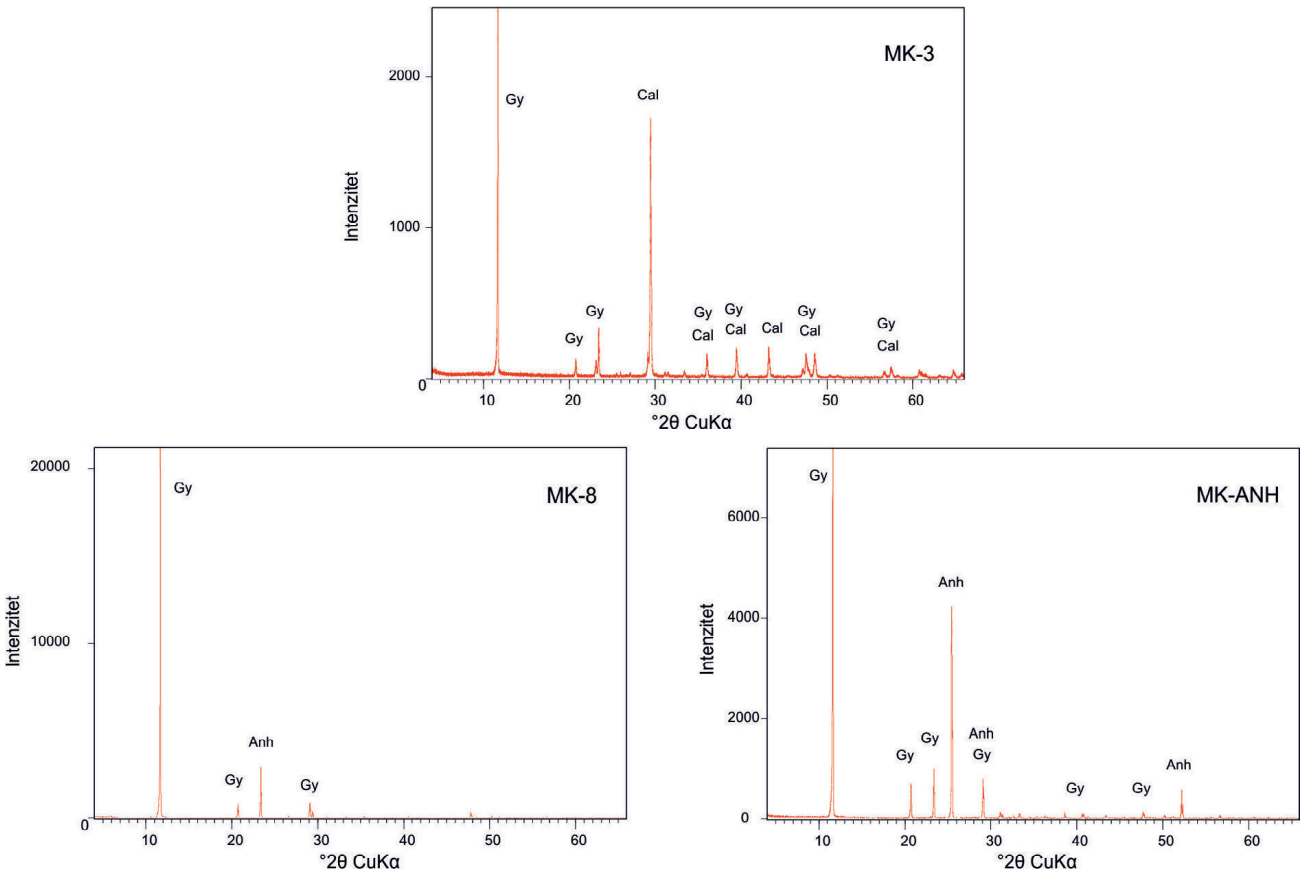

Figure 8. Upper Permian evaporite sample XRD patterns from the Mali Kukor site (i.e., samples MK-3, MK-8, and MK-ANH). Abbreviations: Gp, Gypsum; Cal, Calcite; Anh, Anhydrite.

in addition to gypsum. The data show that dolomite is dominant at the Vranjkovići and Slane Stine sites, while calcite is most abundant at the Mali Kukor site.

Calcite occurs as regular crystals at the Mali Kukor site (Fig. 4; e.g., sample Mk-16) alongside a mass of secondary gypsum that generally exhibits both alabastrine and porphyroblastic textures associated with corroded anhydrite relics. It is thought that this kind of gypsum forms via the replacement of carbonate minerals (i.e., dolomite and calcite) with sulfate-rich solutions. The textural characteristics of this gypsum indicate that carbonate minerals (i.e., calcite or dolomite) were originally replaced by anhydrite, which was in turn replaced by secondary gypsum. Indeed, as this is likely to have been the case, the replacement of carbonate minerals took place at depth under both high temperature and pressure, and favored the formation of anhydrite rather than gypsum (MURRAY, 1964; HOLLIDAY, 1970; KENDALL, 1989; TESTA & LUGLI, 2000, AMADI et al., 2010).

The fact that gypsum occurs locally as lenticular crystals scattered amongst dolomite (Fig. 5) probably indicates that it directly replaced carbonate minerals under near-surface conditions (WARREN, 1999).

The alternation of gypsum and dolomite as couplets continues upwards through the sections studied here and suggests a "dolomite-gypsum rhythmical pattern" at different levels within outcrop successions. Observations show that each couplet comprises a dark-gray, thin-to-thickly bedded dolomite overlain by thickly bedded white gypsum; rhythmic couplets are distinct, but irregularly spaced, and are rich in organic matter when they occur, transitioning upwards into nodular gypsum (Fig. 2).

4.4. Interpretation of different gypsum types

Experimental studies and modern sedimentary analogues indicate that primary gypsum is more commonly precipitated under normal surface conditions (HARDIE, 1967; SHEARMAN, 1985; TESTA & LUGLI, 2000, SCHREIBER & HELMAN, 2005). This means that the anhydrite precursor to this process can be interpreted as a diagenetic product derived from the dehydration of primary gypsum (MURRAY, 1964; HOLLIDAY, 1970, KASPRZYK, 2003); thus, primary gypsum is transformed diagenetically into anhydrite either during burial (MURRAY, 1964; HOLLIDAY, 1970; TESTA & LUGLI, 2000; KIRKLAND, 2003), or via solar heating as was the case for Miocene evaporites in the northwestern Red Sea (AREF et al., 2003). TIŠLJAR (1992) concluded, for example, that evaporitic conditions around the edges of epeiric marine basins tend to exist when general regressive conditions are in place, associated with ongoing coastal seaward progradation.

The microscopic investigations reported here indicate that most of the observed types of secondary gypsum associated with the evaporite units studied resulted from the hydration of precursor anhydrite. The data suggest that all of the types of gypsum seen in evaporite units within the study area (e.g., alabastrine secondary gypsum, porphyroblastic gypsum, fibrous satin spar, and granoblastic gypsum) are of secondary origin, and this observation is confirmed by the widespread presence of satin spar gypsum veins within Upper Permian units. The veins have been considered by many authors to be the result of anhydrite hydration (HOLLIDAY, 1970; KENDALL, 1989; TESTA & LUGLI, 2000). It is therefore thought to be the case that these Upper Perm-

ian evaporite units were originally deposited as gypsum anhydrite? (see below) under restricted shallow marine saline conditions, although this may have varied over time. Additional evidence for this conclusion comes from their regular bedding and the fact that they are interbedded with marine carbonates. During uplift, the exposed parts of these Upper Permian anhydrites were modified to gypsum, although remaining similar to other subsurface examples (ANDREWS, 1992; DALQAMUNI, 1995).

5. CONCLUSION

The mineralogical and petrographic evaluations of evaporitic sediment thin sections presented in this study reveals the characteristics of evaporitic rocks, indicating their primary diagenetic products, and enables a determination of the changes seen throughout the geological evolution of such sediments.

The evaporitic sediments investigated in this study are mainly secondary gypsums that also contain dolomite, anhydrite, muscovite, calcite, quartz, amphibole, and clay minerals. Secondary gypsum can occur in various structural types that range from idiotopic to xenotopic, of which alabastrine, porphyroblastic, and granoblastic types are recognized here alongside a fourth fibrous satin spar structure seen in one sample. Alabastrine and porphyroblastic types most probably correspond to the upper phreatic groundwater zones, while the appearance of gypsum on, or near to, the surface, as well as the presence of anhydrite in deeper parts, reflects the fact that secondary gypsum minerals are the result of anhydrite hydration. This hydration process is initiated at the edges of anhydrite crystal cleavage planes in the form of fibrous satin spar gypsum, especially in tectonically disturbed and cracked zones.

The microscopic and XRD investigations reported in this study reveal that the Upper Permian evaporites at all three sites are primarily composed of microcrystalline secondary gypsum. Indeed, the evaporites at the Vranjkovići and Mali Kukor sites predominantly comprise gypsum with very little anhydrite, while gypsum and anhydrite are present in equal quantities at Slane Stine. Microscopic investigations indicate that most of the gypsum microfacies within these Upper Permian evaporites are the result of parent anhydrite hydration.

The analyses presented in this study also confirm the presence of dolomite and calcite as carbonate minerals. The results of XRD analyses show that dolomite is also present, alongside gypsum and/or anhydrite, at both the Vranjkovići and Slane Stine sites, while calcite dominates at Mali Kukor.

The main conclusion of this study is that the total mineralogical composition of the investigated evaporitic sediments is indicative of several stages of deposition, and that there are key differences between samples from Slane Stine and Vranjkovići and Mali Kukor. The main rock constituent at all sites is gypsum intercalated with dolomite, with the exception of Mali Kukor where a calcite component dominates the lower part of the section.

The Upper Permian evaporite units investigated in this study are mainly composed of microcrystalline secondary gypsum.

ACKNOWLEDGEMENT

This study was supported by The Ministry of Science and Education of the Republic of Croatia Scientific Project: The Map of Mineral Resources of the Republic of Croatia. The authors also wish to thank all those who contributed to the successful completion of this research, especially Erli KOVAČEVIĆ GALOVIĆ from the Croatian Geological Survey, Zagreb, for their assistance, useful comments, and suggestions on this paper.

REFERENCES

ABRANTES JR, F.R., NOGUEIRA, A.C.R. & SOARES J.L. (2016): Permian paleogeography of west-central Pangea: Reconstruction using sabkha-type gypsum-bearing deposits of Parnaíba Basin, Northern Brazil.– Sedimentary Geology, 341, 175–188.

ANDREWS, I. (1992): Permian, Triassic and Jurassic lithostratigraphy in the subsurface of Jordan: natural resources authority of Jordan.– Subsurface Geol. Div., Bull. 4.

AMADI, F.O., MAJOR, R.P. & BARIA, L.R. (2010): Origin of gypsum in deep carbonate rock; primary gypsum vs. rehydrated anhydrite.– Geological Society of America, 42, p.138.

AREF, M., A.M., ABU EL–ENAIN, F.M. & ABDALLAH, G. (2003): Origin of secondary gypsum of the Miocene Abu Dabbab Evaporites, NW Red Sea coast, Egypt.– Fifth International Conference on the Geology of the Middle East, 321–330.

BUTLER, G.P. (1973): Strontium geochemistry of modern and ancient calcium sulphate minerals.– In: PURSER, B.H. (ed.): The Persian Gulf. Holocene Carbonate Sedimentation and Diagenesis in a Shallow Epicontinental Sea. Springer, 423–452.

CROATIAN GEOLOGICAL SURVEY (2009): Geološka karta Republike Hrvatske 1:300.000, izrađena na temelju osnovne geološke karte M 1:100.000, područje Republike Hrvatske [Geological Map of the Republic of Croatia 1:300 000 – in Croatian].– Zagreb.

DALQAMUNI, A. (1995): Sequence stratigraphy and petroleum prospects of the Upper Triassic sediments (Abu Ruweis), North Jordan.– Unpublished MSc thesis, Yarmouk University, Jordan.

DERCOURT, J., RICOU, L.E. & VRIENLINCK, B. (1993): Atlas Tethys – Palaeoenvironmental Maps. Gauthier-Villars, Paris.

DERCOURT, J., GEATANI, M., VRIELINCK, B., BARRIER, E., BIJU-DUVAL, B., BRUNET, M.-F., CADET, J.-P., CRASQUIN, S. & SANDULESCU, M. (ed.), (2000): Atlas Peri-Tethys: Palaeogeographical Maps. CCGM/CGMW, Paris, 24 maps and explanatory notes: XX + 269 pp.

EBERL, D.D. (2003): User guide to RockJock – a program for determining quantitative mineralogy from X-ray diffraction data.– US Geol. Surc. Open File Rep., 03–78.

FORBES, B.G. (1958): Folded Permian Gypsum of Ripon Parks, Yorkshire. Proc. Yorks. Geol. Soc., 31, 351–358.

GABRIĆ, A., ŠINKOVEC, B., SAKAČ, K. & KULJAK, G. (2002): Ležišta gipsa u Republici Hrvatskoj.– Rudarsko-geološko-naftni zbornik, 14, 21–36.

GRIMANI, I., ŠIKIĆ, K. & ŠIMUNIĆ, A. (1962–1966): Osnovna geološka karta SFRJ 1:100000, list Knin L33−141 [*Basic Geological Map of SFRY 1:100000, Knin sheet* – in Croatian].– Geološki zavod, Zagreb, Savezni geološki zavod, Beograd.

GRIMANI, I., JURIŠA, M., ŠIKIĆ, K. & ŠIMUNIĆ, AN. (1975): Tumač Osnovne geološke karte SFRJ, l: 100 000, list Knin, (L-33-141) [*Basic Geological Map of SFRY 1:100000, Geology of the Knin sheet* – in Croatian, English Abstract].– Inst. geol. istraž. Zagreb, Savez. geol. zavod Beograd, 1–61.

HAM, W.E. (1962): Economic Geology and Petrology of Gypsum-Anhydrite Cap Rock, Sulphur Salt Dome, Louisiana.– Mem. Geol. Soc. Am., 50.

HARDIE, L.A. (1967): The gypsum-anhydrite equilibrium at one atmosphere pressure.– Am. Min., 52, 171–200.

HOLLIDAY, D.W. (1970): The petrology of secondary gypsum rocks: A review.– J. Sediment. Petrol., 40, 734–744.

IRWIN, M.L. (1965): General Theory of epeiric clear water sedimentation.– American Association of Petroleum Geologist Bulletin, 49, 445–459.

IVANOVIĆ, A., SIKIRICA, V., MARKOVIĆ, S. & SAKAČ, K. (1977): Osnovna geološka karta SFRJ 1:100000, list Drniš [*Basic Geological Map of SFRY 1:100000, Drniš sheet* – in Croatian].– Geološki zavod, Zagreb, Savezni geološki zavod, Beograd.

IVANOVIĆ, A., SIKIRICA, V. & SAKAĆ, K. (1978): Tumač Osnovne geološke karte SFRJ, l : 100 000, list Drniš, (K 33-9) [*Basic Geological Map of SFRY 1:100000, Geology of the Drniš sheet* – in Croatian, English Abstract].– Inst geol. istraž. Zagreb, Savez. geol. zavod, Beograd.

KASPRZYK, A. (2003): Sedimentological and diagenetic patterns of anhydrite deposits in the Badenian evaporite basin of the Carpathian Foredeep, southern Poland.– Sedimentary Geology, 158, 167–194.

KENDALL, A.C. (1989): Brine mixing in the Devonian of western Canada and its possible significance to regional dolomitization.– Sediment. Geol., 64, 271–285.

KINSMAN, D.L. (1966): Gypsum and anhydrite of recent age, Trucial Coast, Persian Gulf.– Second symposium on salt, Northern Ohio Geol. Soc. Cleveland, 1, 302–326.

KIRKLAND, D.W. (2003): An explanation for the varves of the castile evaporites (upper Permian), Texas and NewMexico,USA.– Sedimentology, 50, 898–920.

KRETZ, R. (1983): Symbols of rock-forming minerals.– American Mineralogist, 68, 277–279.

KULUŠIĆ, A. & BOROJEVIĆ ŠOŠTARIĆ, S. (2014): Dinaride evaporite mélange: Diagenesis of the Kosovo polje evaporates.– Geologia Croatica, 67/1, 59–74. doi: 10.4154/gc.2014.05

LUKŠIĆ, B., CRNOGAJ, S., DEDIĆ, Ž. & JURIĆ, A., (2005): Report on gypsum reserves of the Novo Bulatovo and Pusto groblje quarries of the Kosovo exploitation field.– Unpublished report, Croatian Geological Survey, Zagreb.

MA, B., CAO, Y., ERIKSSON, K.A., JIA, Y. & WANG, Y. (2016): Burial evolution of evaporites with implications for sublacustrine fan reservoir quality: A case study from the Eocene Es4x interval, Dongying depression, Bohai Bay Basin, China.– Marine and Petroleum Geology, 76, 98–114.

MAKLOUF, I.A. & EL-HADDAD, A.A. (2006): Depositional environments and facies of the Late Triassic Abu Ruweis Formation, Jordan.– Journal of Asian Earth Sciences, 28, 372–384.

MOORE, D.M. & REYNOLDS, R.C. (1997): X-ray diffraction and the identification and analysis of clay minerals.– Oxford Univ. Press, Oxford, 378 p.

MURRAY, R.C. (1964): Origin and diagenesis of gypsum and anhydrite.– Journal of Sedimentary Petrology, 34, 512–523.

ORTI, F., PEREZ-LOPEZ, A. & SALANY, J.M. (2017): Triassic evaporites of Iberia; sedimentological and palaeogeographical implications for the western Neotethys evolution during the Middle Triassic-Earliest Jurassic.– Palaeogeography, Palaeoclimatology, Palaeoecology, 471, 157–180.

OGNIBEN, L. (1957): Secondary gypsum of the Sulphur Series, Sicily, and the so-called integration.– Journal of Sedimentary Petrology, 27, 64–79.

PAPEŠ, J., MARINKOVIČ, R., RAIĆ, V., MAGAŠ, N. & SIKIRICA, V. (1968–1980): Osnovna geološka karta SFRJ 1:100000, list Sinj K 33−10 [*Basic Geological Map of SFRY 1:100000, Sinj sheet* – in Croatian].– Geološki zavod, Zagreb, Savezni geološki zavod, Beograd.

RAIĆ, V., PAPEŠ, J., SIKIRICA, V. & MAGAŠ, N. (1984): Tumač Osnovne geološke karte SFRJ, 1:100000, list Sinj (K 33-10). [*Basic Geological Map of SFRY 1:100000, Geology of the Sinj sheet* – in Croatian, English Abstract].– Geoinženjering, Institut za geologiju Sarajevo, Geološki zavod, OOUR za geologiju i paleontologiju. Izd. Savez. geol. zavod, Beograd, l–52.

SCHREIBER, B.C. & HELMAN, M.L. (2005): Criteria for distinguishing primary evaporite features from deformation features in sulfate evaporites.– Journal of Sedimentary Research, 75, 525–533.

SHAW, A.B. (1964): Time in Stratigraphy: New York – McGraw-Hill, 365 p.

SHEARMAN, D.J. (1985): Syndepositional and later diagenetic alteration of primary gypsum to anhydrite.– The Sixth Symposium Salt, the Salt Institute, vol. 1, 44–55.

SHEARMAN, D.J., MOSSOP, G.D., DUNSMORE, H. & MARTIN, M. (1972). Origin of gypsum veins by hydraulic fracture.– Institute of Mining and Metallurgy Transactions (Section B), 81, 149–155.

STROHMENGER, C.J., Al-MANSOORI, A., Al-JEELANI, O., Al-HOSANI, I., Al-SHAMRY, A., SHEBL, H., Al-MEHSIN, K. & Al-BAKER, S. (2008): The arid shallow subtidal to supratidal environment; a case study from the Abu Dhabi Sabkha (United Arab Emirates). Abstracts: Annual Meeting – American Association of Petroleum Geologists, 2008.

ŠUŠNJARA, A., SAKAČ, K., JELEN, B. & GABRIĆ, A. (1992): Upper Permian evaporites and associated rocks of Dalmatia and borderline area of Lika and Bosnia.– Geologia Croatica, 45, 95–114.

TAJ, R.J.A. (2012): Lower Miocene Coastal Lagoon Carbonates and Evaporites of Rabigh Area, Red Sea Coast, Saudi Arabia. Journal of King Abdulaziz University: Marine Sciences, 23, 131–164.

TESTA, G. & LUGLI, S. (2000): Gypsum anhydrite transformation in Messinian evaporites of central Tuscany (Italy).– Sediment. Geol., 249–268.

TIŠLJAR, J. (1992): Origin and depositional environments of the evaporitic and carbonate complex (Upper Permian) from the central part of the Dinarides (Southern Croatia and Westen Bosnia).– Geologia Croatica, 45, 115–126.

TIŠLJAR, J., VLAHOVIĆ, I., VELIĆ, J. & SOKAČ, B. (1992): Carbonate Platform Megafacies of the Jurassic and Cretaceous Deposits of the Karst Dinarides.– Geologia Croatica, 55, 139–170.

VELIĆ, I., VLAHOVIĆ, I. & MATIČEC, D. (2002): Depositional sequences and paleogeography of the Adriatic Carbonate Platform.– Mem. Soc. Geol. Ital., 57, 141–151.

VLAHOVIĆ, I., TIŠLJAR, J., VELIĆ, I. & MATIČEC, D. (2005): Evolution of the Adriatic Carbonate Platform: paleogeography, main events and depositional dynamics.− Palaeogeography, Palaeoclimatology, Palaeoecology, 220, 333–360. doi: 10.1016/j.palaeo.2005.01.011

WARREN, J. (1999): Evaporites: their evolution and economics.– Blackwell Science, Oxford, UK, 438 p.

WARREN, J.K. (2006): Evaporites: sediments, resources and hydrocarbons.– ISBN 3-540-26011-0 Springer Berlin Heidelberg New York, p. 1041.

WATSON, A. (1988): Desert gypsum curst as paleoenviroment indicators: micropetrographic study from southern Tunisia and the central Namib Desert.– J. Arid Environ., 15, 19–42.

WEST, I.M. (1964): Evaporite diagenesis in the Lower Purbeck beds of Dorset.– Geol. Soc. Yorkshire Proc., 34, 315–330.

WEST, I.M. (1965): Macrocell structure and enterlolithic facies in the Visean of Ireland.– Geol. Soc. Yorkshire Proc., 35, 47–58.

WETZEL, A., WEISSERT, H., SCHAUB, M., VOEGLIN, A.R. & FÖLLMI, K. (2013): Sea-water circulation on an oolite-dominated carbonate system in an epeiric sea (Middle Jurassic, Switzerland).– Sedimentology, 60, 19–35.

YESILOVA, P.G. & HELVACI, S. (2013): Diagenesis and paleogeographic development of Oligocene evaporites of the Germik Formation (Kurtalan, SW Siirt), Turkey.– Yerbilimleri, 34, 1–22.

ZAKI, R., WALI, A. & MOSA, M. (2011): Sedimentological and hydrochemical spectrum of recent continental sabkha and signs of its capabilities to generate hydrocarbons: a case study in northwest El Fashn area, Western Desert, Egypt.– Carbonates & Evaporites, 26, 273–286.